Conditioned medium harvested from Hif1α engineered mesenchymal stem cells ameliorates LAD-occlusion -induced injury in rat acute myocardial ischemia model

Article *in* The International Journal of Biochemistry & Cell Biology · December 2020

DOI: 10.1016/j.biocel.2020.105897

CITATIONS
0

READS
37

5 authors, including:

Zahra Alijani
Guilan University of Medical Sciences
2 PUBLICATIONS **1** CITATION
SEE PROFILE

Reza Sabzevari
Guilan University of Medical Sciences
3 PUBLICATIONS **1** CITATION
SEE PROFILE

Amaneh Mohammadi Roushandeh
Hamadan University of Medical Sciences
92 PUBLICATIONS **1,112** CITATIONS
SEE PROFILE

Ali Jahanian-Najafabadi
Isfahan University of Medical Sciences
128 PUBLICATIONS **963** CITATIONS
SEE PROFILE

International Journal of Biochemistry and Cell Biology 130 (2021) 105897

Contents lists available at ScienceDirect

International Journal of Biochemistry and Cell Biology

journal homepage: www.elsevier.com/locate/biocel

Conditioned medium harvested from Hif1α engineered mesenchymal stem cells ameliorates LAD-occlusion -induced injury in rat acute myocardial ischemia model

Zahra Alijani-Ghazyani [a], Amaneh Mohammadi Roushandeh [a,b], Reza Sabzevari [a], Arsalan Salari [c], Mohammad Taghi Razavi Toosi [a], Ali Jahanian-Najafabadi [d], Mehryar Habibi Roudkenar [c,*]

[a] Department of Medical Biotechnology, Faculty of Paramedicine, Guilan University of Medical Sciences, Rasht, Iran
[b] Anatomical Sciences Department, Medicine Faculty, Guilan University of Medical Sciences, Rasht, Iran
[c] Cardiovascular Diseases Research Center, Department of Cardiology, Heshmat Hospital, School of Medicine, Guilan University of Medical Sciences, Rasht, Iran
[d] Department of Pharmaceutical Biotechnology, School of Pharmacy and Pharmaceutical Sciences, Isfahan University of Medical Sciences, Isfahan, Iran

ARTICLE INFO

Keywords:
Myocardial infarction
MSCs
Conditioned medium
HIF-1α
Exogenous overexpression

ABSTRACT

Acute myocardial infarction (AMI) is the most common type of ischemic heart diseases with a high mortality rate. Although recent advances in medical cares and therapies have increased the patient's outcomes, but, still there is no real and effective therapeutic modality for AMI. Hence, development of novel therapeutic strategies is under focus of investigations. MSCs-based therapy has been proposed for AMI, though its efficacy is controversial yet. It is believed that MSCs exert their healing effects via secretion of growth factors/cytokines. However, these cells produce a very minute amount of the factors under normal cultivation. Here, in an attempt to improve the potential therapeutic effect of MSCs-derived conditioned medium (CM) on AMI, we transfected the cells with a recombinant plasmid encoding Hif1α-3A (a mutant form of Hif1α stable under normoxic condition), so Hif1α expression and secretion into CM (MSCs-Hif1α-CM) could be up-regulated under normoxic condition. The therapeutic potential of the MSCs-Hif1α-3A-CM was investigated in a rat model of AMI and compared to the CM harvested from non-manipulated MSCs. Our results showed that the MSCs-Hif1α-3A-CM mitigated MI-induced tissues injury, decreased fibrosis, reduced apoptosis, and limited infarct area size. These findings propose a potential therapeutic strategy for treatment of AMI. However, further preclinical and clinical investigations in this regard are still needed.

1. Introduction

Cardiovascular diseases, including myocardial infarction (MI), are the leading cause of mortality worldwide (Ioacara et al., 2020). MI occurs following reduction in myocardial perfusion commonly due to thrombus formation in a coronary artery, spontaneous coronary artery dissection, or anemia. Necrosis, fibrosis, hypertrophy or apoptosis of cardiomyocytes are the well-known pathological consequences of MI which occur during and/or after it (Sutton and Sharpe, 2000; Talman and Ruskoaho, 2016). It is noteworthy to mention that not only the infracted heart is not capable to renovate itself, but also the available therapeutic modalities are not capable of replacing the damaged cardiac tissue. In fact, currently, there is no real effective treatment for MI. Stem cells-based therapies including the application of mesenchymal stem cells (MSCs) have been proposed for treatment of MI (Behfar et al., 2014). A number of studies reported the ability of MSCs to regenerate infarcted myocardium (Majka et al., 2017; Singh et al., 2016). For instance, immediate injection of MSCs in animal model of MI improved myocardial compliance and ventricular activity, and promoted cardiac nerve sprouting (Berry et al., 2006; Pak et al., 2003; Price et al., 2006). However, there are also some studies that criticize the ability of MSCs to differentiate to cardiomyocytes (Guo et al., 2018; Han et al., 2019).

Abbreviations: AMI, Acute myocardial infarction; MSCs, Mesenchymal stem cells; CM, Conditioned medium; Hif1α, Hypoxia inducible factor 1 alpha; FGF, Fibroblast growth factor; IGF, Insulin like growth factor; VEGF, Vascular endothelial growth factor; LAD, Left anterior descending artery.

* Corresponding author.
E-mail address: roudkenar@gums.ac.ir (M.H. Roudkenar).

https://doi.org/10.1016/j.biocel.2020.105897
Received 25 July 2020; Received in revised form 25 November 2020; Accepted 26 November 2020
Available online 3 December 2020

Furthermore, during isolation, cultivation, and infusion processes, MSCs experience oxidative, nutritional, and shear stresses, hypoxic condition, and unfavorable microenvironment of the recipient tissue such elevated inflammatory cytokines. Altogether, these factors cause dramatical decrease in viability of the transplanted cells (Hao et al., 2017). Supporting this notion, Toma et al. reported that only ~1% of MSCs injected to infarcted heart tissue were viable 24 h post injection, and even this viability decreased to below 0.44 % seventy two hrs later (McGinley et al., 2013; Toma et al., 2002). Therefore, it has been proposed that the therapeutic potential of MSCs is not due to their plasticity, but is related to their paracrine effects (Abbasi-Malati et al., 2018; Madrigal et al., 2014). In other words, the therapeutic potency of MSCs is mainly due to their ability to secrete multiple cytokines, growth factors, and/or peptides which are crucial for tissue regeneration and might be considered a reasonable alternative to MSCs-based therapy (Joyce et al., 2010; Madrigal et al., 2014). The overall secretory factors released to cultivation medium of MSCs is called secretome, and the culture medium is named conditioned medium (CM) (Abbasi-Malati et al., 2018). The usefulness of MSCs derived CM as a therapeutic modality has been shown in a variety of disorders such as brain stroke, neurodegenerative diseases, spinal cord injury, acute and chronic hindlimb ischemia, and myocardial infarction (Baraniak and McDevitt, 2010; Pawitan, 2014). However, under normal cell culture conditions, MSCs produce low levels of secretory factors. Therefore, a number of studies have been conducted to enrich and augment the MSCs derived CM (Amiri et al., 2015). Cultivation of the cells under hypoxic condition is one of the major strategies in this regard (Amiri et al., 2015; McGinley et al., 2013). For example under hypoxic condition, MSCs showed to produce higher levels of growth factors/cytokines such as fibroblast growth factor (FGF), insulin like growth factor (IGF), and vascular endothelial growth factor (VEGF) (Chen et al., 2014), and exhibited protective and angiogenic effects on cardiomyoblasts and endothelial cells, respectively (Burlacu et al., 2013; Cerrada et al., 2013).

It has been well-known that one of the key molecules which are stably expressed in hypoxia is Hypoxia-inducible factor-1 (Hif1) that in turn induces a number of other genes. HIF1 is a heterodimeric protein, consisting of α and β subunits. O_2 concentration is implicated in the regulation of Hif-1α subunit. In fact, normoxic condition results in rapid degradation of Hif1α, whereas hypoxia stabilizes it (Poon et al., 2009; Vaupel and Mayer, 2007). Considering the positive effect of hypoxia on the protective role of the MSCs conditioned medium, and also the fact that HIF1α is one of the key molecule in hypoxic condition, here we first transfected umbilical cord-derived MSCs (hUC-MSCs) by a recombinant construct carrying Hif1α-3A (the Hif1α with three mutations (3A) which makes it stable even under normoxic condition) coding sequence. Next, the conditioned medium of the transfected cells were prepared (MSC-Hif1α-CM) and used in a rat model of MI to investigate its therapeutic potential. When compared to the control (MSC-CM), the MSC-Hif1α-CM protected MI-induced tissue injury, reduced fibrosis, diminished apoptosis, and decreased infarct area size. Therefore, this strategy might be further evaluated in preclinical and clinical studies to be considered as a novel potential treatment for MI.

2. Methods

2.1. Cell culture

hUC-MSCs were isolated as previously described (Amiri et al., 2014). The cells were cultured in low glucose DMEM (Gibco, USA) supplemented with 10 % fetal bovine serum (FBS) (Gibco, USA), and 1% penicillin and streptomycin antibiotics at 37 °C and 5% CO_2. When needed, the cells were sub-cultured by 0.05 % Trypsin-EDTA solution (Gibco, USA).

2.2. Transfection of hUC-MSCs with pcDNA3.1-HIF1α-3A plasmid

The HIF1α-3A coding sequence was sub-cloned from pcDNA4/myc vector (kindly gifted by Hiroshi Harada, Kyoto University, Japan) to pcDNA3.1 plasmid as describe previously (Roudkenar et al., 2020). The recombinant plasmid was designated as pcDNA3.1-HIF1α-3A and used to transfect passage 4 of the hUC-MSCs in 25 cm^2 cell culture flasks at 70–80 % confluency. The transfection was performed by XtremeGENE HP DNA transfection kit (Roche, Germany) using 3 μg/mL of the pcDNA3.1-HIF1-α-3A plasmid according to the manufacture's instruction. As a control, hUC-MSCs were separately transfected with non-recombinant pcDNA3.1 plasmid.

2.3. Assessment of the HIF1α-3A expression by the transfected cells

In order to verify the expression of HIF1α-3A, RT-PCR and western blotting were performed. For the RT-PCR analysis, total RNA was extracted by TRIzol (Invitrogen, USA) reagent as instructed by the manufacturer. Then, cDNA was synthesized using 2 μg of the extracted RNA by a cDNA synthesize kit (Invitrogen, USA). Then, to confirm expression of the HIF1-α-3A mRNA, specific forward (5′-TTGCTAGCATGGAGGGCGCCGGCGGCGC-3′) and reverse (5′-AGTCTAGATCAGTTAACTTGATCCAAAGC3′) primers were used. β-actin mRNA expression was also assessed using forward (5′-TTCTACAATGAGCTGCGTGTGC-3′) and reverse (5′-GTGTTGAAGGTCTCAAACATGAT-3′) primers and used for normalization. The PCR condition included an initial denaturation step at 95 °C for 5 min followed by 30 cycles of 30 s at 95 °C, 30 s at 59 °C, and 60 s at 72 °C, followed by a single step of 5 min at72 °C. Finally, the PCR products were electrophoresed on 1% agarose gel.

In order to confirm the Hif1α-3A protein expression, the hUC-MSCs transfected with either pcDNA3.1-Hif1α-3A or pcDNA3.1 plasmids were lysed and loaded on a 12 % SDS polyacrylamide gel (SDS-PAGE). Then the protein bands were transferred to a PVDF membrane **via** semidry blotting. The membrane was subsequently blocked with 3% skimmed milk and incubated with rabbit anti-Hif1α primary antibody (NB100−105, Novus Biologicals, Littleton, CO, USA). Then the membrane was washed three times and incubated with goat anti-rabbit IgG secondary antibody (H1202, Nichirei Bioscience, Tokyo, Japan). Finally, ECL substrate (Abcam, Cambridge, UK) was added to the membrane, and the protein bands were visualized by ChemiDoc MP imaging system (Biorad, Hercules, CA, USA). Rabbit anti-beta-actin polyclonal antibody (1:3000, Abcam) was used for detection of beta-actin in the cell lysis, as an internal control.

2.4. Preparation, characterization and quality control of the conditioned medium

The hUC-MSCs were washed with PBS 48 h after transfection and further incubated in FBS free medium (L-G DMEM) for 48 h. Thereafter, the culture medium was collected and centrifuged at 1500 *g* to remove cells debris. Then, the supernatant was centrifuged at 5000 *g* for 90 min utilizing centrifugal filter unit with a 3 kDa cut off according to manufacturer's instruction. The prepared CMs (V-CM and HIF1α-3A-CM corresponding to the cells transfected with the pcDNA3.1 or the pcDNA3.1-HIF1α-3A plasmids, respectively) were filtered through a 0·22 μm syringe filter. Finally, the prepared conditioned media were aliquoted in 100 μL portions and lyophilized. The each lyophilized portion was resuspended in 100 μL of PBS, and also serially diluted in PBS to 50 and 25 % (V/V) solutions.

Total protein content of the prepared CMs was determined by BCA protein assay kit according to manufactures' instruction (Sigma, USA), while bovine serum albumin (BSA) was used as standard. Concentration of human vascular endothelial growth factor A (VEGF-A) in the prepared CMs was determined by Human VEGF-A ELISA assay Kit (Abnova, Taiwan) according to the manufacture's protocol.

2.5. Evaluation of the CMs cytotoxicity on H9c2 cell line

H9c2 embryonic rat heart-derived cell line was purchased from national cell bank of Iran (NCBI, Pasteur Institute of Iran, Tehran, Iran). The cells were cultured in DMEM supplemented with 10 % FBS at 37 °C and in a CO_2 incubator. Cytotoxicity of the prepared CMs on H9c2 cells was investigated using MTT assay Kit (KiaZist, Iran). To do this, 7×10^3 cells were seeded in wells of a 96-well plate and treated with three concentrations of 25, 50 and 100 % (V/V) of either V-CM or HIF1-α-CM for 24 h. Then, MTT assay was carried out according to the manufacture's instruction. Finally, the absorbance was read at 570 nm using ELISA micro plate reader. In addition to the MTT assay, trypan blue dye exclusion assay was also performed to evaluate the cells viability and death after treatment with the CMs. In this regard, the cells were trypsinised and then stained with a solution of 0.4 % trypan blue 24 h after treatment with the mentioned concentrations of the CMs. Finally, cell death rate was calculated.

2.6. Acute myocardial infarction model and surgery

All animal experiments were approved by ethical committee of Guilan University of Medical Sciences. Animals were kept at standard animal house at 21−23 °C and 12/12 h light/dark cycle conditions.

Adult male Wistar rats weighing 250−300 g were used in this study. The animals were sedated with 100 mg/kg ketamine and 20 mg/kg xylazine intraperitoneally. To prevent infection, 30 mg/kg Cefazolin was injected to the animals intramuscularly before surgery.

The rats were put in supine position, and their chest was shaved and sterilized by povidone-iodine. The rats were monitored with electrocardiogram throughout the procedure, and to maintain body temperature, they were kept on warm blanket during the surgery. After anesthesia, the animals were intubated using a vein detained needle, and mechanically ventilated using a rodent respirator (NARCO Bio-Systemes, USA). The respiratory rate was set on 70 breaths/min and a tidal volume of 3 mL/100 g body weight. Then, thoracotomy was performed at the 3rd or 4th intercostal space. After dissecting muscles and uncovering heart, the pericardium was removed carefully. MI was induced by permanent ligation of left anterior descending (LAD) artery by 6−0 Prolene suture (SUPA, Iran). The MI was confirmed visually by heart color change (from red to white), and also by changes in electrocardiography which were observed 10 min post-ischemia. The condition of animals were monitored carefully and finally the incisions were closed in layers by continuous sewing (SUPA, Iran).

The animals were divided to five groups including sham group, which subjected to chest opening without induction of ischemia; MI group, in which after opening the chest, the LAD was ligated permanently; MI + PBS group in which 100 μL of PBS was directly injected to four different ischemic areas after infarction; MI + V—CM group which received 100 μL of V-CM(25 % V/V concentration); and MI+Hif1α-3A-CM group which received 100 μL of the HIF1α-3A-CM(25 % V/V concentration) accordingly (The four different points same as MI + PBS).

2.7. Histological studies

The heart of all animals were removed three weeks after surgery and fixed in freshly prepared 4% paraformaldehyde at least for 72 h. The fixed tissues were then paraffin embedded and sectioned at 5 μm thickness. The sections were stained by Hematoxylin and Eosin (H&E) dyes for general morphology detection, and by Masson's trichrome stain to determine the left ventricle (LV) wall thickness and fibrotic area. Fibrosis in the infarct area was measured for three sections of each heart by Image J software (NIH, USA, version 1.8.0_112).

2.8. Apoptosis assay

Apoptosis was detected using in situ cell death detection kit (TAKARA, Japan). Briefly, paraffin embedded sections were deparaffinized by xylene, and antigen retrieval was perform by treatment of the sections with proteinase K (Thermo Scientific, USA) at 37 °C for 20 min. Then, fifty μl of the kit enzyme reaction was added to the sections and incubated at 37 °C for 1 h. In addition, the sections were co-stained with 1 μg/mL DAPI (Sigma, USA) at 37 °C for 20 min. Finally, the cells were observed under fluorescence microscope (Nikon, Japan) and photographed.

2.9. Assessment of infarct area size

Infarct area was determined by triphenyltetrazolium chloride (TTC) method. Briefly, the heart was removed and washed with sterilized normal saline (0.9 %) and frozen at -20. The frozen heart were cut to 2−3 mm sections from apex to bottom using heart matrix and incubated in pre-warmed 1% TTC solution at 37 °C for 30 min. Then, the sections were fixed by formaldehyde solution (10 %) for 2 h. The heart slices were photographed and analyzed with the Image J software.

2.9.1. Statistical analysis

All data were expressed as mean ± SD. Independent experiments were performed to evaluate significant differences between control and other experimental groups. Significant differences were determined by one-way ANOVA and/or two-way ANOVA with the Tukey post-hoc test. All data were analyzed using GraphPad Prism 5 (v5.03, 2009, GraphPad Prism Software Inc., San Diego, CA, USA). P value <0.05 was considered statistically significant.

3. Results

3.1. Overexpression of recombinant HIF1-α in MSCs

To confirm overexpression of the HIF1α-3A mRNA, RT-PCR was performed. As it is represented by Fig. 1, a band of about 2.5 kbp on agarose gel was observed for the cells transfected with the pcDNA3.1-HIF1α-3A plasmid indicating mRNA expression of the gene. However, in case of the cells transfected with pcDNA3.1 no band was observed (Fig. 1, A&B). The expression of HIF1α mRNA was also assessed at different time points post transfection. As it is represented by Supplementary Fig. 1, the highest level of expression was observed 48 h post transfection. Therefore, we considered this time point for later experiments.

Expression and secretion of the HIF1α-3A protein was confirmed by western blotting. As it is shown by Fig. 1.C, the CM harvested from MSCs transfected with the pcDNA3.1-HIF1α-3A plasmid stably expressed HIF1-α-3A protein under normoxic condition and was apparently higher than the basal level of HIF1-α secretion by the cells transfected with the pcDNA3.1 plasmid. In addition, the CM harvested from non-transfected MSCs cultivated under hypoxic condition which was used as a positive control showed significant up-regulation in HIF1-α.

3.2. Harvesting and characterization of conditioned media

The V-CM and HIF1α-3A-CM were harvested from pCDNA3.1 and pcDNA3.1-Hif1α-3A transfected MSCs, respectively, and their total protein concentration was measured by BCA assay. The total protein concentration of Hif1α-3A-CM and V-CM were 335 ± 6 and 220 ± 4 μg/mL, respectively. Furthermore, since VEGF-A gene expression is one of the well-known target of Hif1α (Choi et al., 2011), and also considering its implication in vascularization, the amount of this protein in the harvested CMs was also determined by ELISA. As it is shown by Fig. 2A, the amount of VEGF-A in the Hif1α-3A-CM was considerably higher than in the V-CM, indicating that exogenous and stable expression of Hif1α is capable of inducing its target genes. In addition, this confirmed the functionality of the Hif1α-3A mutant.

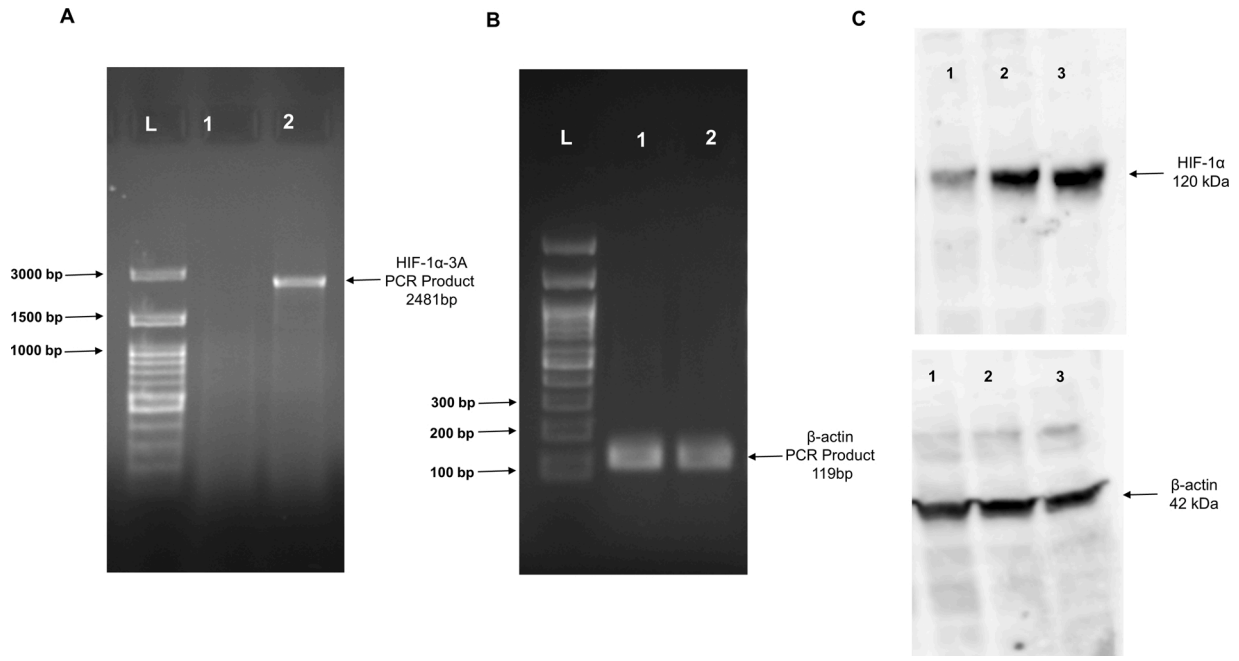

Fig. 1. Assessment of Hif1α-3A expression at mRNA and protein levels. A) RT-PCR analysis of the hUC-MSCs transfected with the pcDNA3.1-HIF1α-3A plasmid confirmed expression of the Hif1α-3A mRNA by revealing a band of about 2481 bp (lane 2), while no band was observed in case of the cells transfected with the pcDNA3.1 plasmid (lane 1). B) Expression of β-actin mRNA in both of the aforementioned cells was also assessed as an internal control for the prepared cDNAs. As it is represented by lanes 1 and 2, the intensity of the amplicon (119 bp) in the two samples is almost the same. L: 100bp standard molecular weight marker. C) Expression of Hif1α/Hif1α-3A protein was assessed by western blotting. Lane 1; MSCs transfected with the pcDNA3.1 and incubated under normoxic condition. Lane 2; MSCs transfected with the pcDNA3.1-Hif1α-3A plasmid and incubated under normoxic condition. Lane3; Non-transfected MSCs cultivated under hypoxic condition (as a positive control for HIF1-α protein expression). As it is shown, expression of the Hif1α-3A protein by the transfected cells was confirmed by showing a band of about 120 kDa. The lower figure represents the expression of β-actin protein as an internal control.

3.3. MSCs derived conditioned medium was not toxic to the H9c2 cells

Cytotoxicity of the CMs was evaluated on H9c2 cells using MTT (Fig. 2B). As it is represented by Fig. 2B, the cells treated with 25 % (V/V) of Hif1α-3A-CM represented a higher OD_{570} than the cells treated with similar amount of the V—CM and also the control (without any treatment) cells ($P < 0.0001$). This could be due to increased metabolic activity and/or cell proliferation. At 50 % V/V concentration, and comparing to the control group, although the Hif1α-3A-CM showed no cytotoxic effects, the V—CM group revealed a significant ($p < 0.0001$) cytotoxicity. At the 100 % V/V concentration, both CMs were prominently cytotoxic to the cells. Furthermore, for confirmation of the MTT results, trypan blue dye exclusion assay was performed (Fig. 2C). The highest viability/lowest cell death was observed in case of treatment of the cells with 25 % V/V concentration of the CMs. At 50 % V/V concentration, the viability of the cells treated with the V—CM was significantly ($p < 0.0001$) lower than the controls. However, no significant difference was observed in case of treatment of the cells with the Hif1α-3A-CM. Finally, at 100 % concentration, both V—CM and Hif1α-3A-CM exhibited significantly ($p < 0.0001$) lower viability/higher cell death compared to the control cells. Interestingly, the number of trypan blue positive cells in V—CM group were significantly ($p < 0.0001$) higher than the Hif1α-3A-CM group. It must be noted that the cytotoxic effect of the CM harvested from non-transfected MSCs was similar to V—CM (data not shown). Hence, we used V—CM for the *in vivo* study.

3.4. Hif1α-3A-CM effectively alleviated LAD occlusion-induced heart tissue damage and decreased fibrosis

AMI was induced by permanent ligation of LAD. Immediately after ligation, the color of the ischemic area changed from red to white which confirmed the lack of blood supply. The AMI was further confirmed by elevation of the ST segment on electrocardiogram (ECG) (data not shown), and serum level of cardiac troponin I (cTnI) which showed a dramatic increase in the MI group 24 h after induction of ischemia. However, its level decreased and reached the normal level after 7 days (Supplementary Fig. 2). As it is shown by Fig. 2.D, the survival rate of the rats was 100 % in the sham, 68.49 % in the MI, 70.12 % in the MI + PBS, 81.23 % in the MI + VC—M, and 91.42 in the MI+HIF1α-CM groups after myocardial infarction. Following administration of CMs, the Hif1α-3A-CM improved the LAD occlusion-induced heart tissue damages in the MI+Hif1α-3A-CM, while high level of infiltration was observed in the MI and MI + PBS groups. It is noteworthy that Aschoff bodies were scattered in the ischemic tissue of MI and MI + PBS groups indicating the inflammation following ischemia (Supplementary Fig. 3). However, no Aschoff bodies were found in the MI+Hif1α-3A-CM group. Moreover, abnormal cardiomyocytes with swollen cytoplasm and pycnotic nucleus were seen in MI and MI + PBS groups, but not in MI+Hif1α-3A-CM group. Also, three weeks after ischemia, considerable left ventricular remodeling was observed in the infarct area of both MI and MI + PBS groups, which resulted in significant ECM degradation, myocardium loss, and progressive infarct scar thinning. However, as shown in Fig. 3, the LV walls in the MI + V—CM and MI+Hif1α-3A-CM groups appeared to be thickened. In addition, injection of V—CM and Hif1α-3A-CM attenuated the LV remodeling especially in the MI+Hif1α-3A-CM group. Analysis of fibrosis that performed by Masson's trichrome staining indicated severe fibrosis in the MI (65.19 ± 10.44 %), MI + PBS (56.76 ± 9.471 %), and even MI + VCM (48.05 ± 10.603 —%) groups. Although, the fibrosis rate was significantly ($p < 0.01$) lower in the MI + V—CM group compared to the MI group, but it was very much lower in the MI+Hif1α—3A-CM group (8.975 ± 6.213), and was significantly ($p < 0.0001$) different with all other groups. In other words, administration of the Hif1α—3A-CM lessened LAD occlusion-induced fibrosis (Fig. 3).

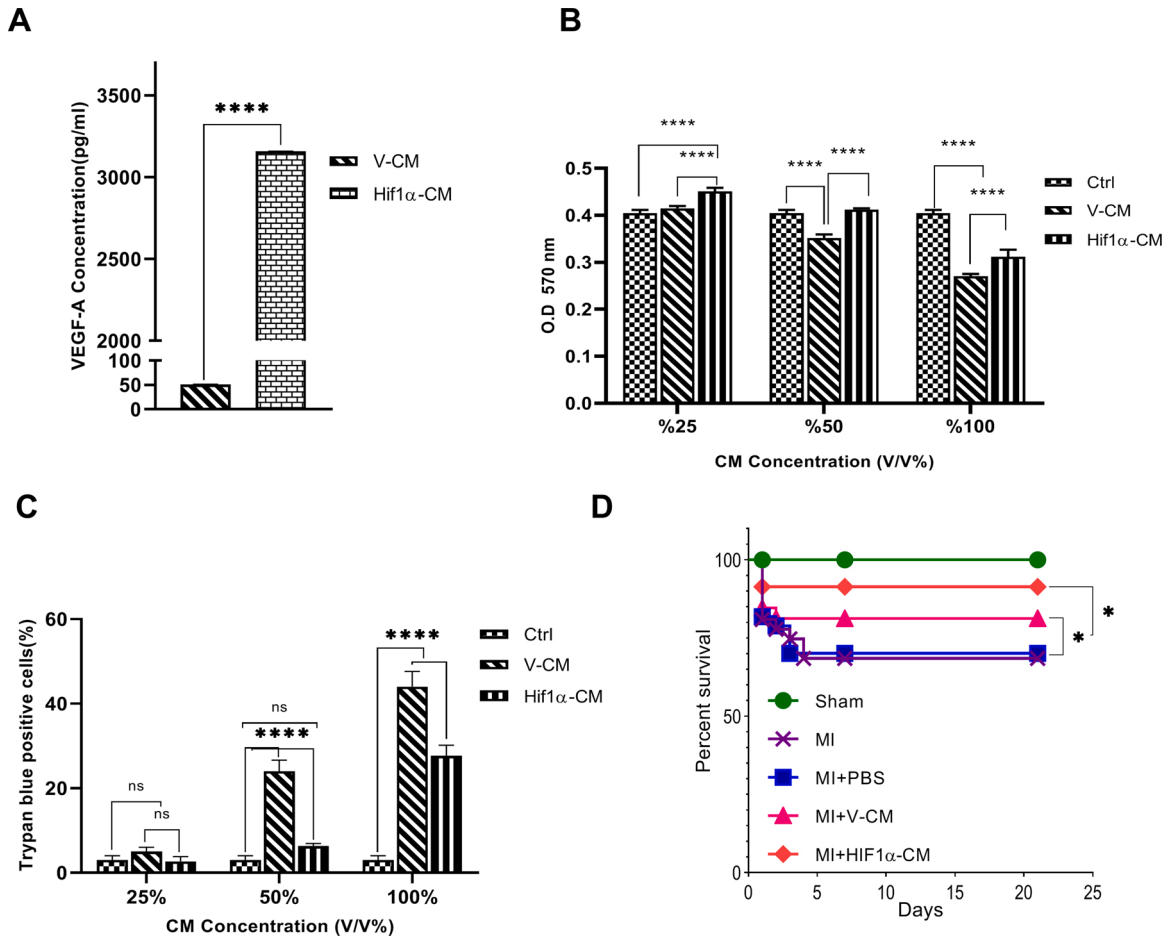

Fig. 2. A) Determination of VEGF-A concentration in the CMs by ELISA method. As it is shown, 48 h post transfection, VEGF-A concentration was significantly much higher in the Hif1α-3A-CM comparing to the V—CM. Data are shown as mean ± SD of three replicates (**** $p < 0.0001$). B) Assessment of cytotoxicity of the prepared CMs by MTT assay. Three concentrations of the CMs (25 %, 50 % and 100 % V/V) were used for treatment of the H9c2 cells for 24 h. Then, the absorbance was measured at OD_{570}. At 100 % (V/V) concentration, both CMs showed significant ($p < 0.0001$) cytotoxicity compared to the non-treated control cells. However, at 25 % (V/V) concentration, V—CM and Hif1α-3A-CM not only showed no toxic effects on the H9c2 cells, but also revealed a slightly higher OD compared to the control. Therefore, the 25 % concentration was selected for the next steps of the study. Data are shown as mean ± SD of three replicates (**** $p < 0.0001$). C) Trypan blue dye exclusion assay was performed 24 h after treatment of the H9c2 cells by three concentrations of the CMs (25 %, 50 % and 100 % v/v). Data are shown as mean ± SD of three replicates (**** $p < 0.0001$). D) Kaplan-Meier curves represented survival rate in the experimental groups. Survival rate was 100 % in sham group, 68.49 % in MI group, 70.12 % in MI + PBS group, 81.23 % in MI + VC—M group, and 91.42 in MI+HIF1α-CM group at on day 21 after myocardial infarction; Log-rank test, $p = 0.030$ compared between MI and MI+HIF1α-CM and $p = 0.040$ compared between MI + PBS and MI+HIF1α-CM (*$p < 0.05$).

3.5. Hif1α-3A-CM reduced LAD occlusion induced apoptotic cell death in cardiomyocytes

Apoptosis was assessed 24 h and one week after injection of CMs. Apoptotic cells were detected in the infarct region of MI, MI + PBS and MI + V—CM groups. Interestingly, the apoptosis was abolished in the ischemic tissue after administration of the Hif1α-3A-CM. As it is shown by Fig. 4, the number of apoptotic cells was significantly higher in the MI, MI + PBS, and MI + V—CM groups compared to the MI+Hif1α3A-CM group ($p < 0.0001$) 24 h after injection. In addition, although the number of apoptotic cells decreased in all groups one week after the CMs administration, but it was still significantly ($p < 0.0001$) higher in all groups compared to the MI+Hif1α-3A-CM group. Altogether, these findings strongly suggested that administration of Hif1α-3A-CM following MI prevents apoptosis of cardiomyocytes.

3.6. Hif1α-3A-CM limited myocardial infarct size

TTC staining was performed to determine the infarct area size three weeks after MI. As it shown by Fig. 5A, the entire apex of the heart is ischemic (white color) in the MI group compared to the MI + V—CM group. Our results revealed that the size of ischemic area in the MI+Hif1α-3A-CM group (10.81 ± 0.158 %) was significantly ($p < 0.0001$) smaller than the MI (27.69 ± 1.531 %), MI + PBS (25.14 ± 3.728), and V—CM (20.44 ± 0.873) groups. It must be noted that V—CM also showed positive effect on limiting the infarct area when compared to the MI ($p < 0.0001$) and MI + PBS ($p < 0.001$) groups (Fig. 5B). In addition, three weeks after ischemia, considerable left ventricular remodeling was observed which resulted in myocardium loss and progressive infarct scar thinning. The quantitative difference in left ventricular thickness of different groups is shown by Fig. 5C. The ventricular thickness was significantly lower in the MI and MI + PBS groups compared to the MI—VC—M ($p < 0.01$) and MI+Hif1α-3A-CM ($p < 0.0001$) groups. Furthermore, the ventricular thickness was significantly ($p < 0.0001$)lower in the MI—VC—M group compared to the control.

4. Discussion

In the current study, we tried to improve the efficacy of MSCs-derived CM and its verification in an animal model of AMI. It has been well known that hypoxia enriches the cytokine/growth factors content of CM, and increases its therapeutic potential (Ferreira et al., 2018). In

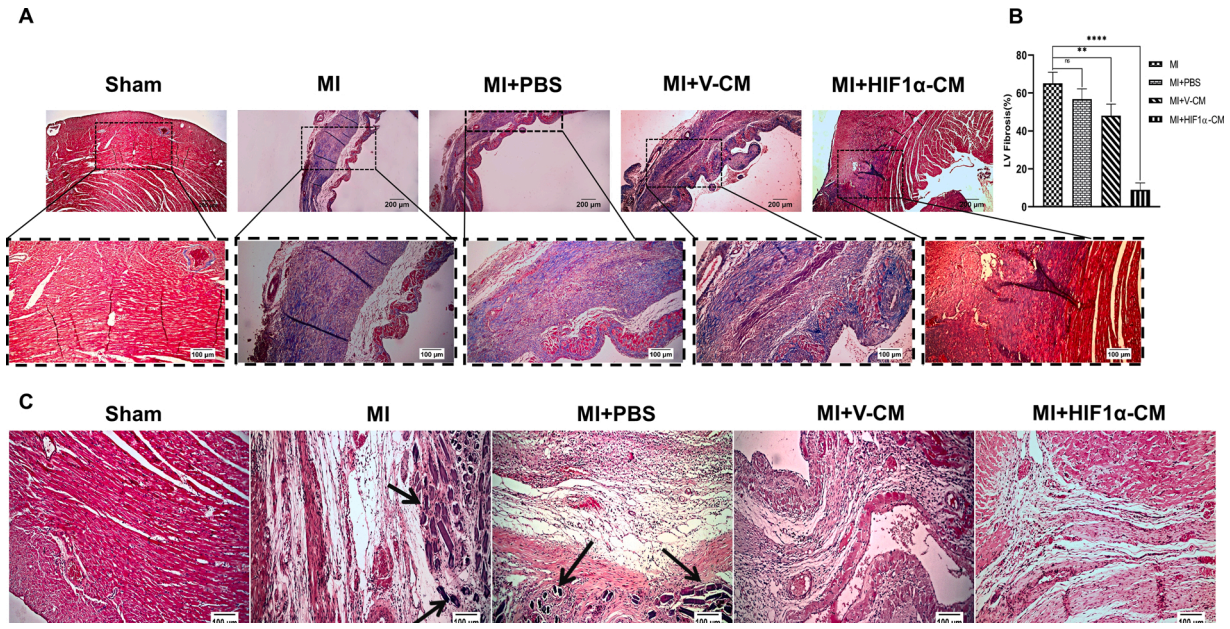

Fig. 3. Morphology and fibrosis of infarcted heart tissues 3 weeks after MI. A) Masson's trichrome stained myocardial sections. Blue, scar tissue; red, viable myocardium. B) Both MI and MI + PBS groups showed a trend towards infarct area expansion while the MI+Hif1α—3A-CM group showed a significant reduction in the infarct area size. This difference was also reflected in the infarct wall thickness which was significantly greater in the MI+Hif1α-3A-CM group than all the other groups. C) H&E staining showed that Hif1α—3A-CM administration attenuated LV remodeling. The presence of Aschoff bodies (arrows). Data are shown as mean ± SD, Number of replicates = 8 (** $p < 0.01$ and **** $p < 0.0001$).

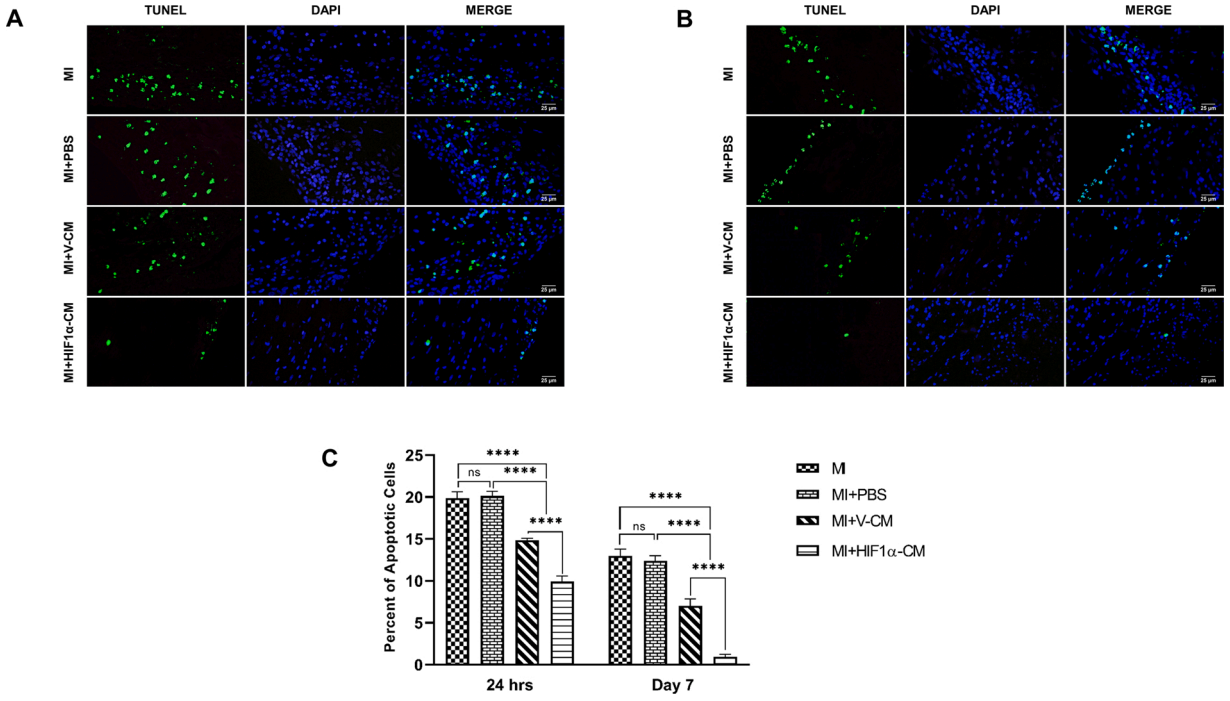

Fig. 4. Detection of apoptosis by TUNEL assay and DAPI staining. The number of apoptotic cardiomyocytes (green cells) 24 h (A) and one week (B) after administration of the CMs was lower in the MI+Hif1α-3A-CM group compared to all other groups. C) The percentage of apoptotic cells in each group at 24 h and one week post CM administration. Data are shown as mean ± SD, Number of replicate = 8 (**** $p < 0.0001$). Hif1α-CM: CM derived from hUC-MSCs transfected with the pcDNA3.1-Hif1α-3A plasmid. V-CM: CM derived from MSCs transfected with the pcDNA3.1 plasmid.

order to explore one of the key molecules expressed under hypoxic condition, HIF1-α, we first transfected the hUC-MSCs by a construct encoding HIF1α-3A. HIF1α-3A is a mutant of HIF1α in which three alanine substitutions in place of proline 402, proline 564, and asparagine 803 made it resistant to normoxic condition (Roudkenar et al., 2020). This stability mimics the expression of Hif1α under hypoxic condition, and so the beneficial roles of this protein could be explored under normoxic condition. According to our *in vitro* results, the Hif1α-3A-CM was toxic to the H9c2 cells at 100 % (V/V) concentration. However, the lowest concentration of the CM, i.e. 25 % (V/V), not only was not toxic to the cells, but also resulted in increased OD_{570}comparing to the controls. This might be due to proliferative effects of the CM,

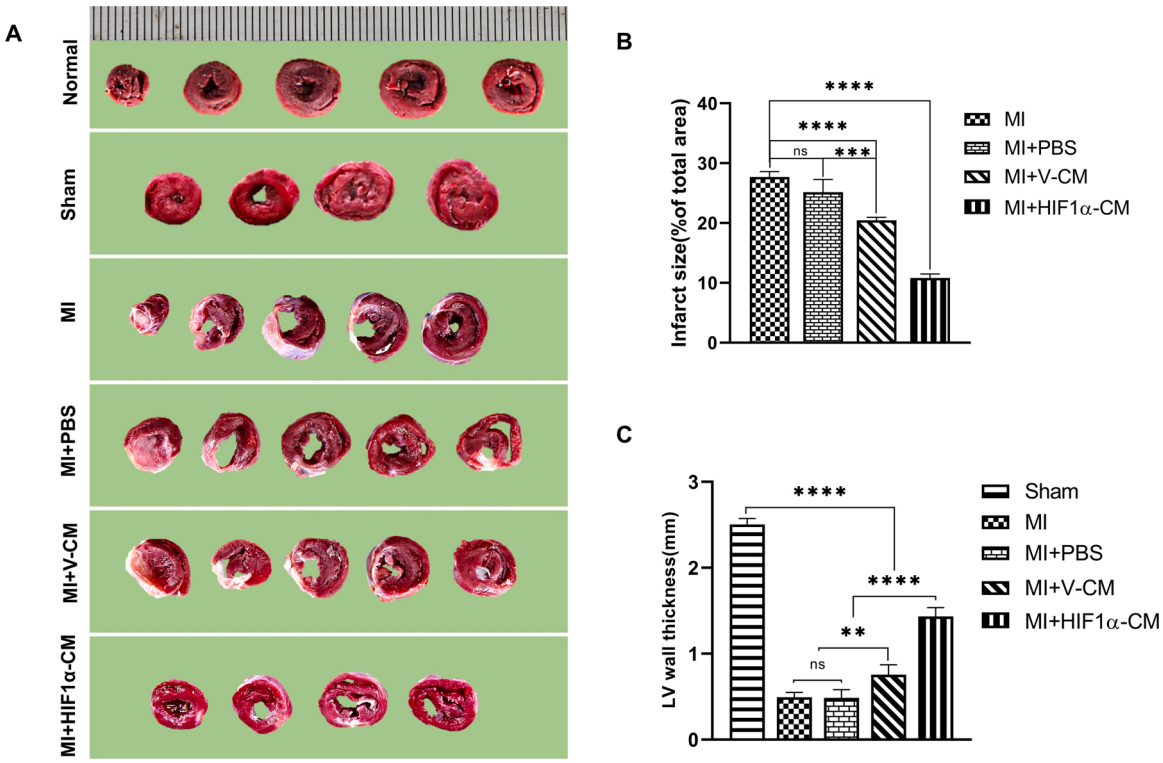

Fig. 5. Assessment of infarct area size. A&B) The size of infarct area in the MI+Hif1α-3A-CM group was significantly ($p < 0.0001$) smaller than the other groups. C) Quantitative analyses of left ventricle wall thickness based on Masson's trichrome staining. The LV wall was significantly thicker in MI and MI + PBS groups than in the MI+HIF1α-CM. Number of replicate = 8.(**$p < 0.01$ and **** $p < 0.0001$). Hif1α-CM: CM derived from hUC-MSCs transfected with the pcDNA3.1-Hif1α-3A plasmid. V-CM: CM derived from MSCs transfected with the pcDNA3.1 plasmid. Data are shown as mean ± SD, Number of replicates = 8 (***$p < 0.001$ and **** $p < 0.0001$).

though it must be further verified by proper experiments such as BrdU assay. In line with this finding, Danieli et al. reported that CM harvested from MSCs under hypoxic condition, increased proliferation of the H9c2 cells (Danieli et al., 2015). It has been reported that hypoxia upregulates a variety of growth factors/cytokines in the MSCs-derived CM. For example He et al. reported that CM harvested from adipose mesenchymal stem cells (ADMSCs) under hypoxic conditions contains higher amounts of hepatocyte growth factor (HGF), stromal derived factor-1 (SDF-1), and particularly VEGF comparing to the normoxic condition (He et al., 2015). Consistent with their findings, we also detected significantly higher amount of VEGF in HIF1α-3A-CM comparing to the V—CM. The increased level of VEGF also indicates that the exogenously overexpressed Hif1α is functionally active, and can up-regulate its target genes under normoxia. It must be noted that Hif1α is the main regulator of angiomodulatory function of MSCs under hypoxia (Cerrada et al., 2013; Razban et al., 2012; Rosová et al., 2008). We next, examined the therapeutic effects of Hif1α-3A-CM in a rat model of AMI. Our results revealed that the administration of CMs mitigated LAD occlusion-induced heart tissue damages and this effect was prominent in the Hif1α-3A-CM group.

MSCs-based therapy has been proposed for MI (Han et al., 2019; Musiał-Wysocka et al., 2019). Nevertheless, the activity and survival of injected MSCs are low which results in inefficacy of the therapy (Toma et al., 2002). It has been proved that the injected MSCs face harsh environments (such as host immune reactions and oxidative stress), and high shear stress during and post transplantation (Choe et al., 2019; Hao et al., 2017). Recently, it has been shown that therapeutic effects of MSCs are mediated by their paracrine effects (Abbasi-Malati et al., 2018; Madrigal et al., 2014). On the other hand, subsequent to the hypoxic condition caused by MI, HIF-1α is stably induced to exert its cytoprotective functions (Gupta and Ashraf, 2018). Therefore, by exogenous expression of the Hif1α-3A, we potentiated the corresponding CM like what is naturally occurred in MI. Our result revealed that the Hif1α-3A-CM ameliorated the LAD-occlusion induced heart tissue damages. In addition, since no Aschoff bodies were detected in the MI-Hif1α-3A-CM group, it seems that the Hif1α-3A-CM exerts anti-inflammatory effects. It is worth mentioning that following myocardial ischemia the cardiomyocytes undergo necrosis, apoptosis and autophagy (Eltzschig and Carmeliet, 2011). In addition, immune responses result in inflammation and recruitment of immune cells and infiltration and finally increases the infarct size and remodeling of left ventricle (Arslan et al., 2011; Ong et al., 2018). It seems that the Hif1α-3A-CM could exert its therapeutic effects through anti-inflammatory properties. Supporting this notion, it has been reported that systemic injection of MSCs-derived exosomes decreased tissue macrophages, inflammatory chemokines and cytokines (Sun et al., 2018). Furthermore, MSCs-derived CM inhibited the pro-inflamatory factors including IFN-γ, TNF-α, and increased the anti-inflammatory factors such as IL-10 (Caplan, 2007; Yi and Song, 2012). Moreover, MSCs and/or MSCs-derive CM have immunomodulatory effects on not only macrophages, but also on other immune cells including B cells, natural killer, dendritic, and mast cells (Rad et al., 2019). Our findings showed declined inflammation in ischemic hearts that received MSCs-CM particularly in the HIF1α-3A-CM group. In addition, the infiltration was also dramatically decreased in the HIF1α-3A-CM as well.

In other words, our findings suggest that HIF1α-3A-CM restored the ischemic heart tissue by immunomodulatory effects which resulted in observation of no Aschoff bodies. However, this warrants further investigations including evaluation of pro-/anti-inflammatory cytokines in the CM.

In a rat model of MI, Selvasandran et al. showed that TNF-α and hypoxia-induced secretome harvested from rat bone marrow-derived mesenchymal stem cells (rBM-MSCs) results in a considerably higher left ventricle fractional shortening in comparison to the control group

(Selvasandran et al., 2018). Fibrotic scars of the cardiac muscle are well-known pathological consequences of MI (Cleutjens et al., 1995). Furthermore, fibrosis is the most common cause of morbidity and mortality due to MI (Pfeffer and Braunwald, 1990; Sun, 2009). Therefore, any therapeutic intervention which decreases the fibrosis is advantageous. Interestingly, our results showed that the administration of Hif1α-3A-CM considerably limits the fibrosis following MI.

A number of studies have shown that apoptosis play an important role in AMI (Krijnen et al., 2002; Teringova and Tousek, 2017). Apoptosis has been detected predominantly in the peri-infarcted region and significantly contributes to myocyte death in AMI (Hu et al., 2008). Therefore, we investigated whether administration of Hif1α—3A-CM is able to abolish LAD occlusion-induced apoptosis. Within our assumption, the administration of Hif1α-3A-CM resulted in considerable reduction in apoptotic cell death, which was even significantly higher than the anti-apoptotic effect of V-CM.

Danieli et al. also demonstrated that infusion of CM harvested from amniotic membrane-derived mesenchymal stromal cells (hAMCs) into the infarcted heart decreases the infarct size, enhances capillary formation at the infarct border zone, and diminishes cardiomyocyte apoptotic death and ventricular remodeling (Danieli et al., 2015). He et al. also demonstrated that CM harvested from ADMSCs under hypoxic condition decreased the infarct size (He et al., 2015). Here we also investigated the effect of the prepared CMs on infarct size. Conspicuously, we found that although both V—CM and Hif1α-3A-CM limited the myocardial infarct size, the reduction was prominent in the Hif1α-3A-CM group. Consistent with our findings, the reduction in infarct size by administration of CMs harvested from MSCs with a variety of sources has been also reported previously (Danieli et al., 2015; Timmers et al., 2008). Though further studies remain to be investigated to clarify the precise mechanisms underlying MSCs-Hif1α-3A-CM protective effects, the potential mechanisms could be: (1) Hif1α-3A-CM may regulate cell migration in response to MI; (2) Hif1α-3A-CM may act as a chemoattractant to recruit some potential specific cell type for regeneration; and (3) Hif1α-3A-CM may reduce oxidative-induced cardiomyocytes death and even stimulate their proliferation. Supporting this notion, it has been shown that MSCs secret a variety of molecules including VEGF that contribute in cardiac repair during ischemia (Huang et al., 2014; Shan et al., 2018; Sid-Otmane et al., 2020; Zhang et al., 2018). It is worth mentioning that VEGF expression is directly regulated by HIF-1α. Our findings also revealed that VEGF concentration was significantly higher in the HIF1α-3A-CM. This high level of VEGF might result in more neomyoangiogenesis and formation of new vessels in heart. This, in turn, can provide sufficient blood flow to restore the cardiomyocytes, inhibit apoptosis, and prevent the destructive changes in the early phase of left ventricular remodeling. It has been reported that secretion of VEGF by MSCs stimulates the mobilization of c-kit^{+} cells from injured heart or distant regions (Wang et al., 2017). Altogether, some growth factors/cytokines/peptides in the MSCs-derived CM such as VEGF more probably exert their restorative potential through modulation of immune responses, suppression of apoptosis, and stimulation of angiogenesis.

CM has several advantages over MSCs such as easy harvesting and preparation, being freezable and packageable which makes it easy to transport, suitable for repeated administration and potential allogenic applications (Vizoso et al., 2017),? These are the potentioal advantage of our prepared Hif1α-3A-CM for future clinical application as well. However, currently there is not any standard GMP regulation for its validations and methods of preparation. Therefore, further investigations in this regard are needed. It is worth mentioning that although we showed Hif1α-3A-CM exhibited protective effects on MI, we had the limitation to perform echocardiography to evaluate the improvement of heart function following administration of the CM. In the current study, we prepared the CM from UC-MSCs by overexpression of Hif1α-3A. Application of other cell sources such as ADMSCs, rBM-MSCs, and AMCs to generate the same/similar results with HIF1a-3A overexpression could also be possible, however, it needs further investigation.

5. Conclusion

In the current study, we suggest a novel potential therapeutic agent for MI. However, further and comprehensive studies are still required to define potential mechanisms underlying the Hif1α-3A-CM protective effects. Moreover, in order to clinically use the CM, further studies such as investigation of its safety and therapeutic effects must be performed in larger animal model and clinical trials.

Ethical approval

All experimental procedures were approved by the Institutional Animal Careand Use Committee *(IACUC) at* Guilan University of Medical Sciences.

CRediT authorship contribution statement

Zahra Alijani-Ghazyani: Methodology, Formal analysis, Writing - original draft. **Amaneh Mohammadi Roushandeh:** Methodology, Supervision, Writing - review & editing. **Reza Sabzevari:** Methodology. **Arsalan Salari:** Writing - review & editing. **Mohammad Taghi Razavi Toosi:** Methodology. **Ali Jahanian-Najafabadi:** Formal analysis, Writing - review & editing. **Mehryar Habibi Roudkenar:** Conceptualization, Writing - review & editing, Supervision, Funding acquisition.

Declaration of Competing Interest

The authors declare that they have no conflict of interest.

Acknowledgement

This study was supported by research deputy of Guilan University of Medical Sciences (Grant number: IR.GUMS.REC.1396.508).

Appendix A. Supplementary data

Supplementary material related to this article can be found, in the online version, at doi:https://doi.org/10.1016/j.biocel.2020.105897.

References

Abbasi-Malati, Z., Roushandeh, A.M., Kuwahara, Y., Roudkenar, M.H., 2018. Mesenchymal stem cells on horizon: a new arsenal of therapeutic agents. Stem Cell Rev. Rep. 14 (4), 484–499.

Amiri, F., Halabian, R., Salimian, M., Shokrgozar, M.A., Soleimani, M., Jahanian-Najafabadi, A., Roudkenar, M.H., 2014. Induction of multipotency in umbilical cord-derived mesenchymal stem cells cultivated under suspension conditions. Cell Stress Chaperones 19 (5), 657–666.

Amiri, F., Jahanian-Najafabadi, A., Roudkenar, M.H., 2015. In vitro augmentation of mesenchymal stem cells viability in stressful microenvironments. Cell Stress Chaperones 20 (2), 237–251.

Arslan, F., De Kleijn, D.P., Pasterkamp, G., 2011. Innate immune signaling in cardiac ischemia. Nat. Rev. Cardiol. 8 (5), 292.

Baraniak, P.R., McDevitt, T.C., 2010. Stem cell paracrine actions and tissue regeneration. Regen. Med. 5 (1), 121–143.

Behfar, A., Crespo-Diaz, R., Terzic, A., Gersh, B.J., 2014. Cell therapy for cardiac repair—lessons from clinical trials. Nat. Rev. Cardiol. 11 (4), 232.

Berry, M.F., Engler, A.J., Woo, Y.J., Pirolli, T.J., Bish, L.T., Jayasankar, V., Morine, K.J., Gardner, T.J., Discher, D.E., Sweeney, H.L., 2006. Mesenchymal stem cell injection after myocardial infarction improves myocardial compliance. Am. J. Physiol. Heart Circul. Physiol. 290 (6), H2196–H2203.

Burlacu, A., Grigorescu, G., Rosca, A.-M., Preda, M.B., Simionescu, M., 2013. Factors secreted by mesenchymal stem cells and endothelial progenitor cells have complementary effects on angiogenesis in vitro. Stem Cells Dev. 22 (4), 643–653.

Caplan, A.I., 2007. Adult mesenchymal stem cells for tissue engineering versus regenerative medicine. J. Cell. Physiol. 213 (2), 341–347.

Cerrada, I., Ruiz-Saurí, A., Carrero, R., Trigueros, C., Dorronsoro, A., Sanchez-Puelles, J. M., Diez-Juan, A., Montero, J.A., Sepúlveda, P., 2013. Hypoxia-inducible factor 1

alpha contributes to cardiac healing in mesenchymal stem cells-mediated cardiac repair. Stem Cells Dev. 22 (3), 501–511.
Chen, L., Xu, Y., Zhao, J., Zhang, Z., Yang, R., Xie, J., Liu, X., Qi, S., 2014. Conditioned medium from hypoxic bone marrow-derived mesenchymal stem cells enhances wound healing in mice. PLoS One 9 (4).
Choe, G., Kim, S.-W., Park, J., Park, J., Kim, S., Kim, Y.S., Ahn, Y., Jung, D.-W., Williams, D.R., Lee, J.Y., 2019. Anti-oxidant activity reinforced reduced graphene oxide/alginate microgels: mesenchymal stem cell encapsulation and regeneration of infarcted hearts. Biomaterials 225, 119513.
Choi, S.B., Park, J.B., Song, T.-J., Choi, S.Y., 2011. Molecular mechanism of HIF-1-independent VEGF expression in a hepatocellular carcinoma cell line. Int. J. Mol. Med. 28 (3), 449–454.
Cleutjens, J., Verluyten, M.J., Smiths, J.F., Daemen, M.J., 1995. Collagen remodeling after myocardial infarction in the rat heart. Am. J. Pathol. 147, 325–338.
Danieli, P., Malpasso, G., Ciuffreda, M.C., Cervio, E., Calvillo, L., Copes, F., Pisano, F., Mura, M., Kleijn, L., De Boer, R.A., 2015. Conditioned medium from human amniotic mesenchymal stromal cells limits infarct size and enhances angiogenesis. Stem Cells Transl. Med. 4 (5), 448–458.
Eltzschig, H.K., Carmeliet, P., 2011. Hypoxia and inflammation. N. Engl. J. Med. 364 (7), 656–665.
Ferreira, J.R., Teixeira, G.Q., Santos, S.G., Barbosa, M.A., Almeida-Porada, G., Gonçalves, R.M., 2018. Mesenchymal stromal cell secretome: influencing therapeutic potential by cellular pre-conditioning. Front. Immunol. 9, 2837.
Guo, X., Bai, Y., Zhang, L., Zhang, B., Zagidullin, N., Carvalho, K., Du, Z., Cai, B., 2018. Cardiomyocyte differentiation of mesenchymal stem cells from bone marrow: new regulators and its implications. Stem Cell Res. Ther. 9 (1), 44.
Gupta, N., Ashraf, M.Z., 2018. Hypoxia Signaling in Cardiovascular Diseases, Hypoxia and Anoxia. IntechOpen.
Han, Y., Li, X., Zhang, Y., Han, Y., Chang, F., Ding, J., 2019. Mesenchymal stem cells for regenerative medicine. Cells 8 (8), 886.
Hao, T., Li, J., Yao, F., Dong, D., Wang, Y., Yang, B., Wang, C., 2017. Injectable fullerenol/alginate hydrogel for suppression of oxidative stress damage in brown adipose-derived stem cells and cardiac repair. ACS Nano 11 (6), 5474–5488.
He, J., Cai, Y., Luo, L., Liu, H., 2015. Hypoxic adipose mesenchymal stem cells derived conditioned medium protects myocardial infarct in rat. Eur. Rev. Med. Pharmacol. Sci. 19 (22), 4397–4406.
Hu, X., Yu, S.P., Fraser, J.L., Lu, Z., Ogle, M.E., Wang, J.-A., Wei, L., 2008. Transplantation of hypoxia-preconditioned mesenchymal stem cells improves infarcted heart function via enhanced survival of implanted cells and angiogenesis. J. Thorac. Cardiovasc. Surg. 135 (4), 799–808.
Huang, B., Qian, J., Ma, J., Huang, Z., Shen, Y., Chen, X., Sun, A., Ge, J., Chen, H., 2014. Myocardial transfection of hypoxia-inducible factor-1α and co-transplantation of mesenchymal stem cells enhance cardiac repair in rats with experimental myocardial infarction. Stem Cell Res. Ther. 5 (1), 1–16.
Ioacara, S., Popescu, A.C., Tenenbaum, J., Dimulescu, D.R., Popescu, M.R., Sirbu, A., Fica, S., 2020. Acute myocardial infarction mortality rates and trends in Romania between 1994 and 2017. Int. J. Environ. Res. Public Health 17 (1), 285.
Joyce, N., Annett, G., Wirthlin, L., Olson, S., Bauer, G., Nolta, J.A., 2010. Mesenchymal stem cells for the treatment of neurodegenerative disease. Regen. Med. 5 (6), 933–946.
Krijnen, P., Nijmeijer, R., Meijer, C., Visser, C., Hack, C., Niessen, H., 2002. Apoptosis in myocardial ischaemia and infarction. J. Clin. Pathol. 55 (11), 801–811.
Madrigal, M., Rao, K.S., Riordan, N.H., 2014. A review of therapeutic effects of mesenchymal stem cell secretions and induction of secretory modification by different culture methods. J. Transl. Med. 12 (1), 260.
Majka, M., Sułkowski, M., Badyra, B., Musiałek, P., 2017. Concise review: mesenchymal stem cells in cardiovascular regeneration: emerging research directions and clinical applications. Stem Cells Transl. Med. 6 (10), 1859–1867.
McGinley, L.M., McMahon, J., Stocca, A., Duffy, A., Flynn, A., O'Toole, D., O'Brien, T., 2013. Mesenchymal stem cell survival in the infarcted heart is enhanced by lentivirus vector-mediated heat shock protein 27 expression. Hum. Gene Ther. 24 (10), 840–851.
Musiał-Wysocka, A., Kot, M., Majka, M., 2019. The pros and cons of mesenchymal stem cell-based therapies. Cell Transplant. 28 (7), 801–812.
Ong, S.-B., Hernández-Reséndiz, S., Crespo-Avilan, G.E., Mukhametshina, R.T., Kwek, X.-Y., Cabrera-Fuentes, H.A., Hausenloy, D.J., 2018. Inflammation following acute myocardial infarction: multiple players, dynamic roles, and novel therapeutic opportunities. Pharmacol. Ther. 186, 73–87.
Pak, H.N., Qayyum, M., Kim, D.T., Hamabe, A., Miyauchi, Y., Lill, M.C., Frantzen, M., Takizawa, K., Chen, L.S., Fishbein, M.C., 2003. Mesenchymal stem cell injection induces cardiac nerve sprouting and increased tenascin expression in a Swine model of myocardial infarction. J. Cardiovasc. Electrophysiol. 14 (8), 841–848.
Pawitan, J.A., 2014. Prospect of stem cell conditioned medium in regenerative medicine. Biomed Res. Int. 2014.
Pfeffer, M.A., Braunwald, E., 1990. Ventricular remodeling after myocardial infarction. Experimental observations and clinical implications. Circulation 81 (4), 1161–1172.
Poon, E., Harris, A.L., Ashcroft, M., 2009. Targeting the hypoxia-inducible factor (HIF) pathway in cancer. Expert Rev. Mol. Med. 11.
Price, M.J., Chou, C.-C., Frantzen, M., Miyamoto, T., Kar, S., Lee, S., Shah, P.K., Martin, B.J., Lill, M., Forrester, J.S., 2006. Intravenous mesenchymal stem cell therapy early after reperfused acute myocardial infarction improves left ventricular function and alters electrophysiologic properties. Int. J. Cardiol. 111 (2), 231–239.
Rad, F., Ghorbani, M., Roushandeh, A.M., Roudkenar, M.H., 2019. Mesenchymal stem cell-based therapy for autoimmune diseases: emerging roles of extracellular vesicles. Mol. Biol. Rep. 46 (1), 1533–1549.
Razban, V., Lotfi, A.S., Soleimani, M., Ahmadi, H., Massumi, M., Khajeh, S., Ghaedi, M., Arjmand, S., Najavand, S., Khoshdel, A., 2012. HIF-1α overexpression induces angiogenesis in mesenchymal stem cells. Biores. Open Access 1 (4), 174–183.
Rosová, I., Dao, M., Capoccia, B., Link, D., Nolta, J.A., 2008. Hypoxic preconditioning results in increased motility and improved therapeutic potential of human mesenchymal stem cells. Stem Cells 26 (8), 2173–2182.
Roudkenar, M.H., Fukumoto, M., Roushandeh, A.M., Kuwahra, Y., Uroshihara, Y., Harada, H., Fukumoto, M., 2020. Disturbance in the regulation of miR 17-92 cluster on HIF-1-α expression contributes to clinically relevant radioresistant cells: an in vitro study. Cytotechnology 1–13.
Selvasandran, K., Makhoul, G., Jaiswal, P.K., Jurakhan, R., Li, L., Ridwan, K., Cecere, R., 2018. A tumor necrosis factor-α and hypoxia-induced secretome therapy for myocardial repair. Ann. Thorac. Surg. 105 (3), 715–723.
Shan, S., Liu, Z., Guo, T., Wang, M., Tian, S., Zhang, Y., Wang, K., Zheng, H., Zhao, X., Zuo, P., 2018. Growth arrest-specific gene 6 transfer promotes mesenchymal stem cell survival and cardiac repair under hypoxia and ischemia via enhanced autocrine signaling and paracrine action. Arch. Biochem. Biophys. 660, 108–120.
Sid-Otmane, C., Perrault, L.P., Ly, H.Q., 2020. Mesenchymal stem cell mediates cardiac repair through autocrine, paracrine and endocrine axes. J. Transl. Med. 18 (1), 1–9.
Singh, A., Singh, A., Sen, D., 2016. Mesenchymal stem cells in cardiac regeneration: a detailed progress report of the last 6 years (2010–2015). Stem Cell Res. Ther. 7 (1), 82.
Sun, Y., 2009. Myocardial repair/remodelling following infarction: roles of local factors. Cardiovasc. Res. 81 (3), 482–490.
Sun, X., Shan, A., Wei, Z., Xu, B., 2018. Intravenous mesenchymal stem cell-derived exosomes ameliorate myocardial inflammation in the dilated cardiomyopathy. Biochem. Biophys. Res. Commun. 503 (4), 2611–2618.
Sutton, M.G.S.J., Sharpe, N., 2000. Left ventricular remodeling after myocardial infarction: pathophysiology and therapy. Circulation 101 (25), 2981–2988.
Talman, V., Ruskoaho, H., 2016. Cardiac fibrosis in myocardial infarction—from repair and remodeling to regeneration. Cell Tissue Res. 365 (3), 563–581.
Teringova, E., Tousek, P., 2017. Apoptosis in ischemic heart disease. J. Transl. Med. 15 (1), 87.
Timmers, L., Lim, S.K., Arslan, F., Armstrong, J.S., Hoefer, I.E., Doevendans, P.A., Piek, J. J., El Oakley, R.M., Choo, A., Lee, C.N., 2008. Reduction of myocardial infarct size by human mesenchymal stem cell conditioned medium. Stem Cell Res. 1 (2), 129–137.
Toma, C., Pittenger, M.F., Cahill, K.S., Byrne, B.J., Kessler, P.D., 2002. Human mesenchymal stem cells differentiate to a cardiomyocyte phenotype in the adult murine heart. Circulation 105 (1), 93–98.
Vaupel, P., Mayer, A., 2007. Hypoxia in cancer: significance and impact on clinical outcome. Cancer Metastasis Rev. 26 (2), 225–239.
Vizoso, F.J., Eiro, N., Cid, S., Schneider, J., Perez-Fernandez, R., 2017. Mesenchymal stem cell secretome: toward cell-free therapeutic strategies in regenerative medicine. Int. J. Mol. Sci. 18 (9), 1852.
Wang, Ql., Wang, Hj., Li, Zh., Wang, Yl., Wu, Xp., Tan, Yz., 2017. Mesenchymal stem cell-loaded cardiac patch promotes epicardial activation and repair of the infarcted myocardium. J. Cell. Mol. Med. 21 (9), 1751–1766.
Yi, T., Song, S.U., 2012. Immunomodulatory properties of mesenchymal stem cells and their therapeutic applications. Arch. Pharm. Res. 35 (2), 213–221.
Zhang, S., Zhao, L., Wang, J., Chen, N., Yan, J., Pan, X., 2018. HIF-2 α and Oct4 have synergistic effects on survival and myocardial repair of very small embryonic-like mesenchymal stem cells in infarcted hearts. Cell Death Dis. 8 (1), e2548.